The Role of Phase Equilibria in AlN Sintering

M. Medraj[1] and R.A.L. Drew[2]

[1]Concordia University, Montreal, Quebec, Canada

[2]McGill University, Montreal, Quebec, Canada

Keywords: AlN-Al_2O_3-Y_2O_3 phase diagram; Thermodynamic modeling; Neutron diffraction, AlN.

Abstract: Thermodynamic and phase diagram data were critically assessed for all phases in the AlN-Al_2O_3, Al_2O_3-Y_2O_3 and AlN-Y_2O_3 systems from room temperature to above the liquidus temperatures at atmospheric pressure. All these data were optimised to obtain a set of model parameters for Gibbs energy of the liquid and all solid phases as function of composition and temperature. The ternary phase diagram of the AlN-Al_2O_3-Y_2O_3 was developed by Gibbs energy minimization using interpolation procedures based on modeling the binary subsystems. The resultant phase diagram was verified experimentally at selected compositions using *in situ* high temperature neutron diffractometry. These experimental results agree with the thermodynamic calculations of AlN-Al_2O_3-Y_2O_3. The ternary phase diagram has been constructed for the first time in this work. Moreover, high temperature neutron diffractometry has permitted real time measurement of the reactions involved in this ternary system, especially to determine the temperature range for each reaction, which would have been difficult to establish by other means. Liquid-phase sintering of AlN with Y_2O_3 as an additive has been studied and compared with the thermodynamic results. Sintering was performed in the temperature range of 1750-1950°C for up to four hours under a N_2 atmosphere to optimise the sintering conditions for each composition. The relative density exceeded 95% for all the compositions sintered at 1850°C and full densification was achieved for all four compositions sintered at 1900°C. The microstructure and assemblage of the secondary phases have a significant effect on the final thermal conductivity of the sintered AlN. Thermodynamic modelling of AlN-Al_2O_3-Y_2O_3 system provided an important basis for understanding the sintering behaviour and interpreting the experimental results.

Introduction

Yttria (Y_2O_3) is the best additive for AlN sintering. AlN densifies by a liquid phase mechanism, where the surface oxide/oxynitride (mostly alumina) reacts with Y_2O_3 to form a Y-Al-O-N liquid that promotes particle rearrangement and densification. Construction of the phase relations in this multicomponent system is essential for optimizing the properties of AlN. To date, there is little information on the ternary AlN-Al_2O_3-sintering additives system [1] and in spite of the large interest attracted in the recent years by the excellent properties of AlN sintered by Y_2O_3, no attempts have been made up to now to construct the AlN-Al_2O_3-Y_2O_3 ternary phase diagram. To calculate reliable ternary, quaternary, and higher order metallic and ceramic phase diagrams, we need thermodynamic description of the binary phase diagrams and a thermodynamic model that can extrapolate binary data reliably into ternary and higher-order systems [2]. This is commonly done for metals where the thermodynamic data are more readily available. For ceramic systems, thermodynamic data are very sparse. Furthermore measurements are very difficult considering the high temperatures involved.

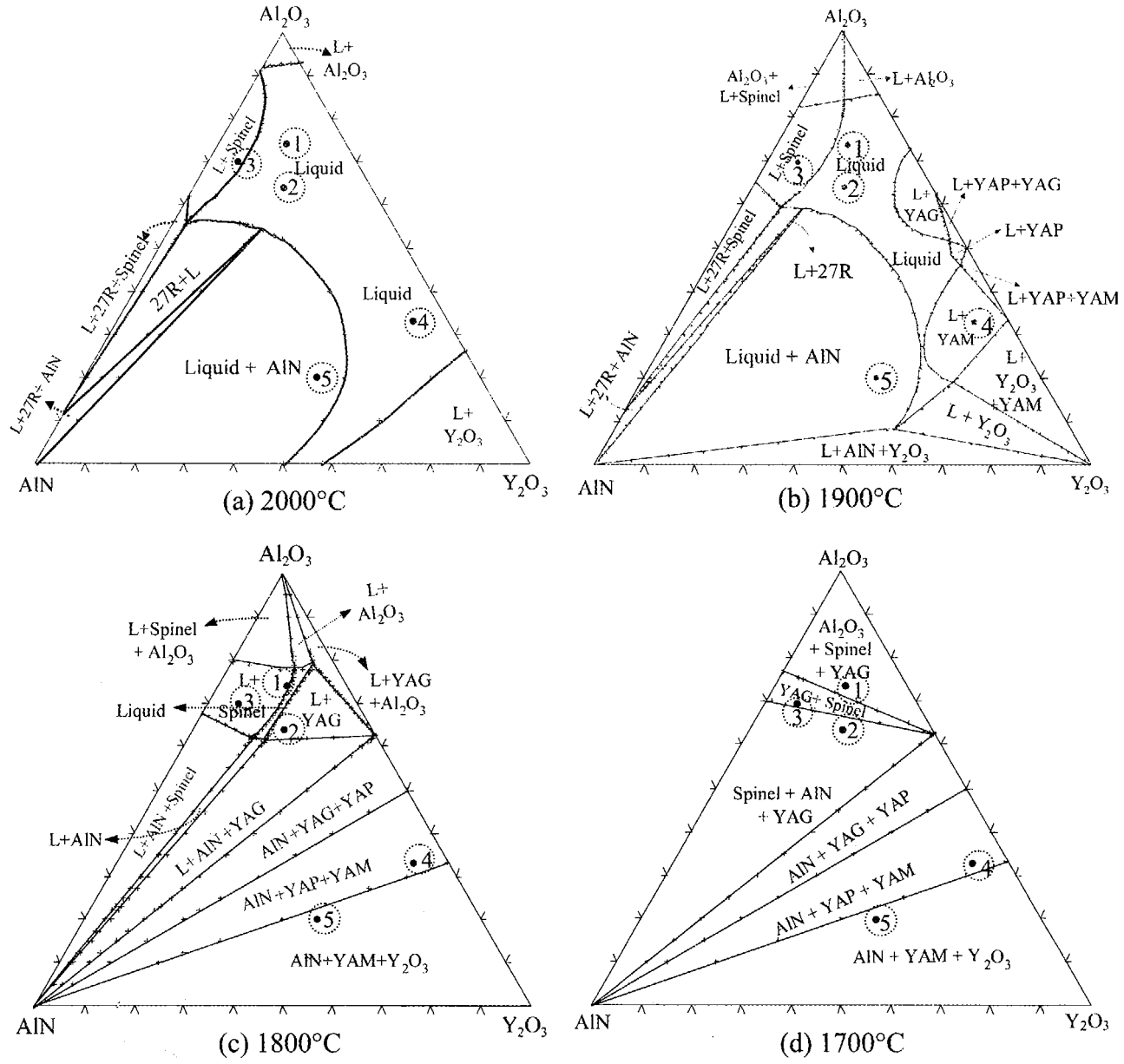

Fig. 1: Isothermal sections of AlN-Al_2O_3-Y_2O_3 with the investigated ternary compositions.

Thermodynamic Modeling of AlN-Al_2O_3-Y_2O_3 System

There is an increasing demand for the development of thermodynamic databases, which are practically useful. A database for AlN-Al_2O_3-Y_2O_3 system was built using the F*A*C*T system [3]. Details of the thermodynamic modeling and the experimental investigation of the system using *in situ* neutron diffraction were published earlier [4,5].

The storage, retrieval and manipulation of thermodynamic data with the aid of the computer require accurate analytical representation of thermodynamic properties of phases. Values of the standard Gibbs energies, G^o, of each component are entered and stored in the solution database along with parameters which define the Gibbs energy of mixing according to Kohler/Toop polynomial model. In the present treatment the ternary excess Gibbs energy was calculated solely from a binary data interpolation. The ternary phase

diagrams were calculated by taking all the thermodynamic data stated for the binary phases into consideration. The calculated isothermal sections of AlN-Al_2O_3-Y_2O_3 system are given in Fig. 1.

Experimental Procedure

Materials: AlN powder, Grade F (Tokuyama Soda, Japan) containing <0.9 wt% of oxygen, <400 ppm of carbon, and trace amounts of other impurities (<60 ppm of Ca, <10 ppm of Fe, <15 ppm of Si), was used. The powder had a mean particle size of <0.3 μm and a specific surface area of 3.3 m^2/g. The Al_2O_3 powder, Grade A16-SG (Alcoa Industrial Chemical Division, Canada) with 99.8% purity was used. The Y_2O_3 powder, Grade 5630X (Union Molycorp, U.S.A.) had a mean agglomerate size of 1.8 μm and specific surface area of 33 m^2/g.

Neutron Diffraction: To investigate the phase evolution in AlN-Al_2O_3-Y_2O_3 system experimentally, neutron diffraction patterns were acquired *in situ* at elevated temperature using the DUALSPEC high-resolution powder diffractometer, C2, at the NRU reactor of Atomic Energy of Canada Limited (AECL) Chalk River Laboratories. The diffractometer is an 800-channel position sensitive detector that spans 80° in scattering angle, 2θ. The wavelength, λ, of the neutron beam was calibrated by measuring the diffraction pattern of a standard powder of alumina, obtained from the National Institute of Standards and Technology. λ = 1.33(1) Å and 2θ range from 8° to 88° were used in this experiment. The diffractometer was equipped with a tantalum-element vacuum furnace capable of reaching temperatures as high as 2000°C.

AlN, Y_2O_3 and Al_2O_3 powder were mixed in various stoichiometric amounts. Table 1 and Fig. 1 show the composition of these samples.

Table 1: The chemical composition of the samples studied by neutron diffraction.

Sample No.	Composition [mol%]		
	AlN	Al_2O_3	Y_2O_3
1	12	74	14
2	17.5	64	18.5
3	24	70	6
4	7	33	60
5	33	20	47

In situ neutron diffraction was performed during heating and cooling of these samples by monitoring the changes in the diffraction peaks and the diffraction angles. In this paper composition 1, only, will be discussed. Detailed experimental investigation of the ternary system is in [5]. A neutron diffraction spectrum for each sample was collected at room temperature to form the reference for any reactions taking place upon heating. The evolution of the reactions was followed by incrementally raising the temperature, and maintaining it for 120 min. to ensure that the reaction was complete. Also, cooling was carried out in steps to detect the crystallization as well as the stability of each phase. Heating and cooling profiles were determined for each sample according to critical points, which were predicted by the thermodynamic calculations. The samples were heated in nitrogen gas to prevent the decomposition of AlN.

AlN Sintering: The amount of Y_2O_3 required as a sintering additive depends on the quantity of oxygen present in the AlN powder. The total oxygen level in the AlN powder was analysed after milling and drying. The AlN powder was mixed with various amounts of Y_2O_3 powder as shown in Table 2. The pre-mixed compositions were ball milled in a plastic container for 24 hours using 3 mm diameter ZrO_2 media and reagent grade isopropanol with a solid to liquid ratio of 1:5 by volume. After milling for 24 hours, the mixtures of AlN and Y_2O_3 were dried in a microwave oven to completely remove the isopropanol. The mixtures were then granulated

through a 212 μm mesh sieve and were then uniaxially and isostatically pressed to form discs 32 mm in diameter, and a thickness of 3 mm.

Table 2: Amount of Y_2O_3 in the samples studied by sintering.

Composition	Y_2O_3 Content [wt%]
I	1.36
II	3.04
III	3.47
IV	7.59

All sintering experiments were performed in a horizontal, graphite element resistance furnace equipped for inert atmosphere and the temperature was controlled using a type C thermocouple. The green compacts were placed on a BN setter and then sintered in N_2 at 1700-1950°C for various hold times followed by furnace cooling. Densities of the sintered AlN compacts were measured by the Archimedes' principle according to a modified version of the ASTM standard C373-72. The theoretical densities were determined by pycnometry; four representative sintered AlN ceramics from each composition were crushed into powder, and then the volume of each powder was measured in a 10 mL pycnometer bottle with isopropanol. The theoretical density was then calculated using the weight and volume of the powders. The powders were phase analysed using filtered CuKα X-ray radiation. The thermal conductivity measurements of AlN specimens were performed by the Laser-flash technique using a thermal diffusivity measurement facility (Microflash NDT) utilizing a spatially uniform single pulse from a CO_2 laser.

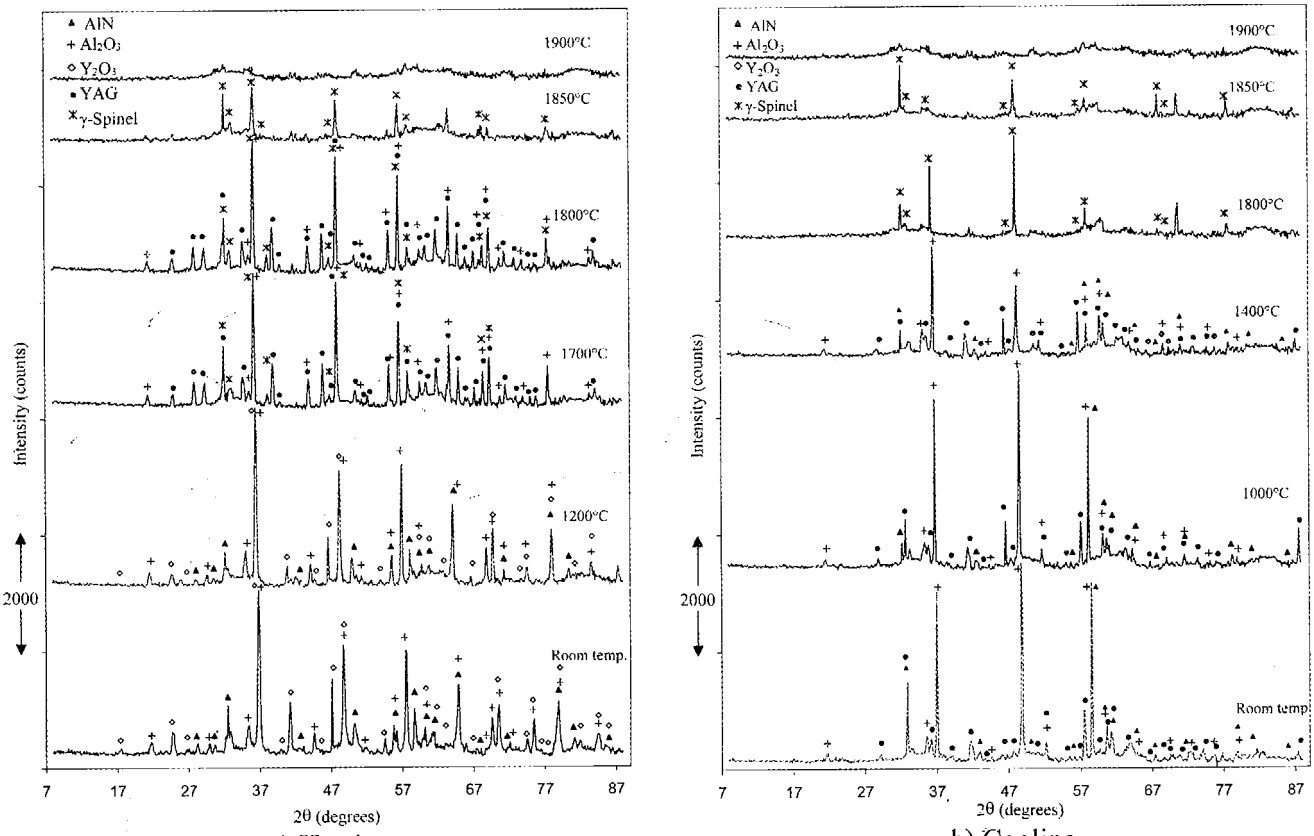

a) Heating b) Cooling

Fig. 2: Neutron diffractograms of composition 1(12 AlN, 74 Al_2O_3 and 14 mol% Y_2O_3).

Results and Discussion

Diffraction patterns obtained during heating and cooling of composition 1 are shown in Fig. 2. The patterns are shifted by a suitable offset for better comparison. The peaks are identified by markers as given in the legend of each figure, and will be discussed and compared with the thermodynamic findings in this section. The effect of thermal expansion was observed in all the samples when the peaks shifted to lower and higher diffraction angles due to heating and cooling, respectively.

Increasing the temperature to 1200°C did not introduce any change in the neutron diffraction pattern and indicates that no reaction took place in this temperature range. The first changes were visible when comparing the neutron diffraction patterns at 1200°C and that at 1700°C, where additional peaks appeared and were found to belong to YAG and γ-spinel. Unlike Al_2O_3 diffraction peaks, Y_2O_3 peaks were not observed at 1700°C, this means that all the 14 mol% Y_2O_3 reacted to produce the YAG phase, whereas residual Al_2O_3 shows incomplete reaction to form γ-spinel. This is consistent with the ternary phase diagram shown in Fig. 1 (d) where composition 1 lies in the three-phase-region of Al_2O_3, γ-spinel and YAG. Cheng *et al.* also observed incomplete reaction between Al_2O_3 and AlN at 1650°C for 6 h. They noticed an increase in the amount of γ-spinel with increasing time from 1 to 6 h [6]. Moreover, Yawei *et al.* [7] concluded that it is difficult to produce γ-spinel by reaction sintering below 1650°C.

Upon heating from 1700°C to 1800°C, no difference in the diffraction patterns was observed. Neutron diffraction patterns were acquired at higher temperatures to detect liquid formation and melting. At 1850°C YAG was not observed, whereas γ-spinel was present. And, since no other peaks were present at this temperature, it can be concluded that liquid formation started between 1800°C and 1850°C. This is consistent with the isothermal section calculated at 1800°C (Fig. 1(c)).

It can be seen from Fig. 2(a) that this composition lost crystallinity and became liquid at 1900°C, hence melting occurred between 1850°C and 1900°C, and is consistent with the calculated isothermal section at 1900°C shown in Fig. 1(b).

Fig. 2(b) shows the cooling cycle for composition 1. It can be seen that γ-spinel was crystallized by 1850°C, confirming that the liquidus is in the temperature range of 1850°C to 1900°C. By cooling to 1400°C, decomposition of γ-spinel phase had occurred. This is evident by the new peaks of AlN and Al_2O_3 detected at this temperature. YAG peaks were observed in the diffraction pattern collected at 1400°C. The same phases were found at 1000°C but with stronger peaks for AlN and Al_2O_3, indicating further decomposition of γ-spinel upon cooling. The patterns obtained at 1000°C and at room temperature are similar and are composed of AlN, YAG and Al_2O_3 upon reaching room temperature.

Fig. 3 shows the effect of temperature on the sintering of AlN for the compositions under consideration. Basically all compositions reach complete densification after sintering at 1850°C for one hour. The experimental results can be

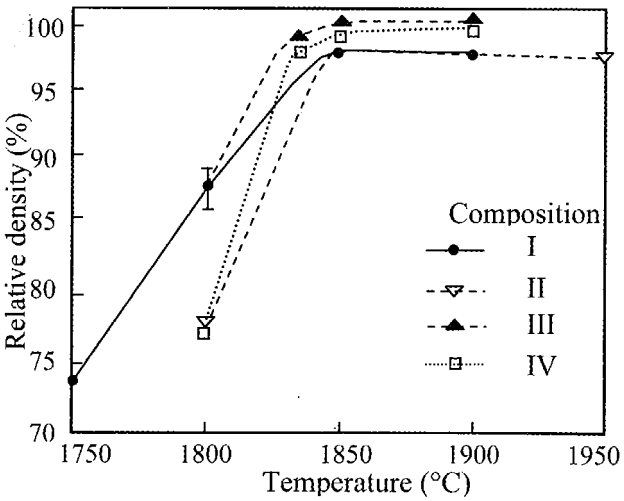

Fig. 3: Relative density as a function of sintering temperature [8].

explained by the phase amount charts shown in Fig. 4. These diagrams show that all compositions would have formed liquid at this temperature. The liquid promoted the densification noticed in the sintered samples. Also, Fig. 3 shows that composition I reached higher density than the other compositions at 1800°C, this can be explained by Fig. 4(a). This figure indicates that this composition starts forming liquid at 1782°C whereas the other compositions required higher temperature to form liquid. In all cases sintering reaches completion within one hour for sintering at 1900°C because liquid readily exists in all the compositions at this temperature as can be seen in Fig. 4.

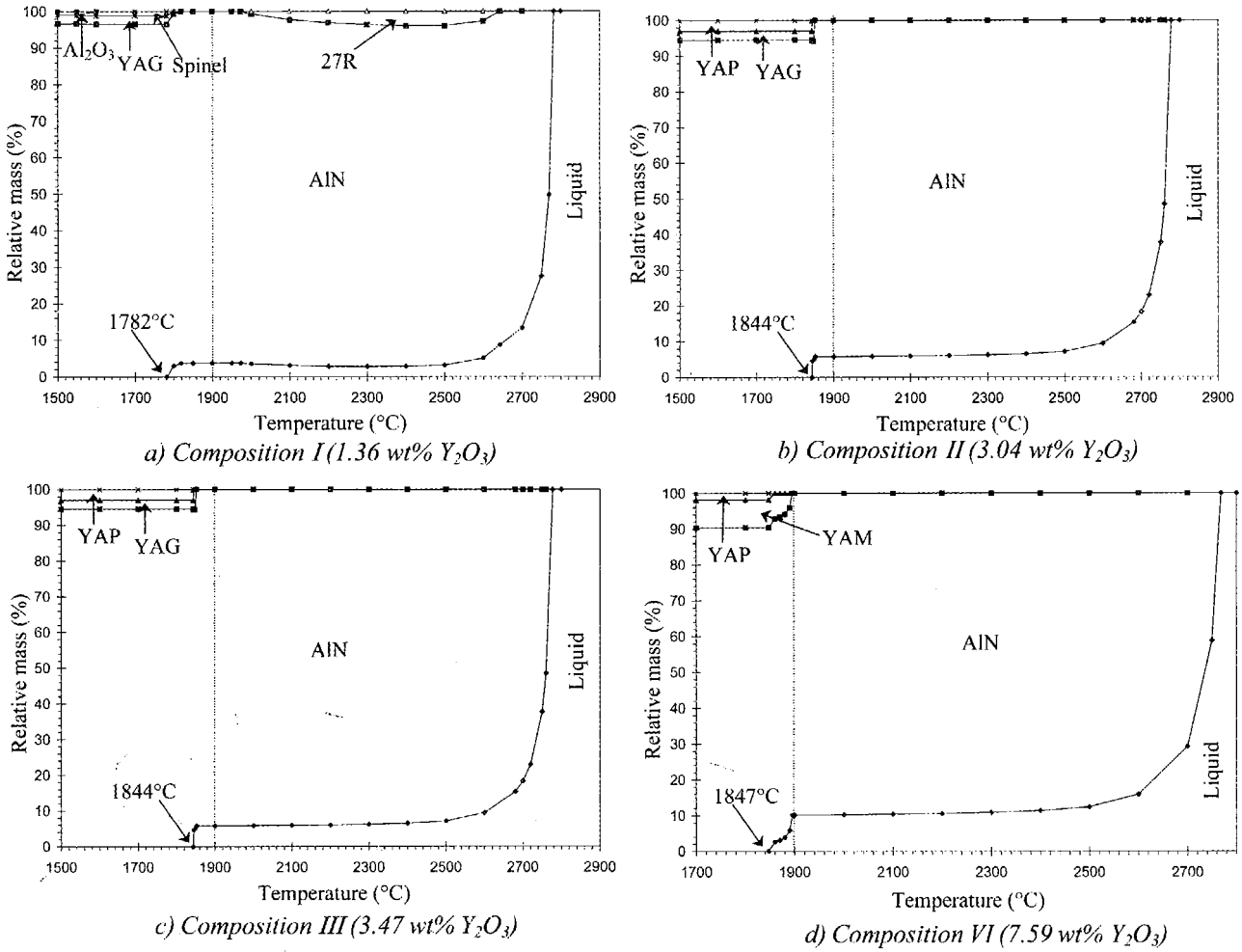

a) Composition I (1.36 wt% Y_2O_3)

b) Composition II (3.04 wt% Y_2O_3)

c) Composition III (3.47 wt% Y_2O_3)

d) Composition VI (7.59 wt% Y_2O_3)

Figure 4: Phase amounts charts for AlN sintered samples

Fig. 4(a) shows, that at room temperature, composition I consists of 96.64 wt% AlN in addition to 2.38 wt% YAG and 0.976 wt% Al_2O_3. The X-ray diffraction at room temperature in Fig. 5(a) show peaks for AlN and YAG phases only. Al_2O_3 peaks were not detected because the amount of residual Al_2O_3 is very small and below the detection limit of the equipment. Moreover, oxide/oxynitride occurs as a thin surface layer on the original AlN particles. Because of this, a secondary phase and residual γ-spinel occur as grain boundary films after sintering and so the thermal conductivity is very low for this sample, as can be seen in Fig. 6. This occurred because the amount of added Y_2O_3 was insufficient to fully react with residual Al_2O_3 and to purify the AlN and to complete the oxygen removal from both the lattice and the

grain surfaces. Fig. 4(b) shows that at room temperature composition II consists of 94.96 wt% AlN, 3.65 wt% YAG and 1.39 wt% YAP. In this sample there is more YAG than YAP at room temperature. This agrees with the X-ray pattern shown in Fig. 5(b) where YAG peaks are stronger than those of YAP phase. Fig. 5(c) indicates that composition III has a similar phase assemblage to composition II with a difference in the relative amount of each phase. At room temperature, composition III consists of 94.53 wt% AlN, 2.52 wt% YAG and 2.95 wt% YAP. This corresponds well with the X-ray pattern for this sample shown in Fig. 5(c). Fig. 4(d) shows the phase assemblage for composition IV and at room temperature this sample is composed of 90.41 wt% AlN, 7.75 wt% YAM and 1.84 wt% YAP. This sample has more YAM than YAP, which agrees with Fig. 5(d), where the diffraction peaks for YAM were stronger than for YAP.

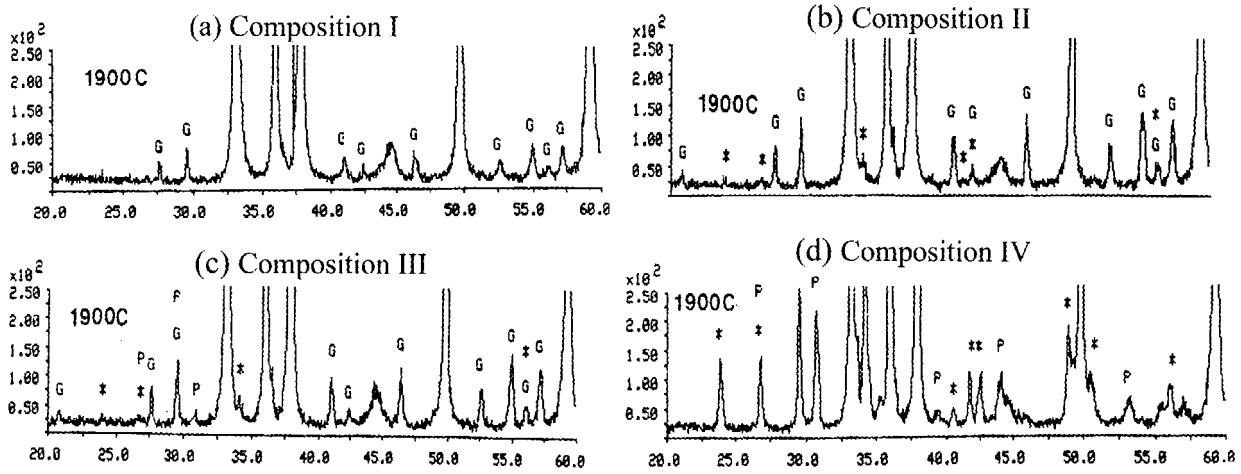

*Fig. 5: X-ray powder diffraction patterns of the four compositions, G: YAG, P: YAP and *: YAM.*

Fig. 5 gives the X-ray powder diffraction patterns for the four compositions after sintering at 1900°C for one hour. Each composition shows strong peaks associated with AlN in addition to minor peaks associated with the secondary phases. These results agree well with the thermodynamic calculations presented in Fig. 4.

The addition of Y_2O_3 appears to have a further effect on changing the wetting behaviour of the liquid phase with respect to the AlN grains. Indeed the dihedral angle of the secondary phase at the grain junction is high (>70°). This has a significant effect on the thermal conductivity. Jackson *et al.* [9] suggest that thermal conductivity rises to a maximum and then decreases due to the increase in volume fraction of aluminates with further Y_2O_3 addition. Fig. 6 shows the trend in thermal conductivity of the four compositions along with their relative densities. As discussed above, the amount of secondary phase increases with Y_2O_3 content, thus there is an optimum additive level. The thermal conductivity of the aluminate phase is low (<10W/m.K), hence as the volume fraction increases, a decrease in the overall thermal conductivity is expected. The thermal conductivity of AlN sintered without Y_2O_3 has a significantly lower value of 65 W/m.K than material sintered with Y_2O_3.

Therefore, the effect of the additive has a major impact on the conductivity in two ways: (a) it removes oxygen from the AlN particle surface during sintering and (b) a microstructural change occurs as the aluminate de-wets the grain boundaries and segregates to the grain junctions leading to AlN-AlN grain boundary contact. This figure shows, also, that compositions II, III and IV have higher thermal conductivity than composition I because the

oxide layer, in these three samples, was consumed to produce YAG, YAP and YAM as secondary phases.

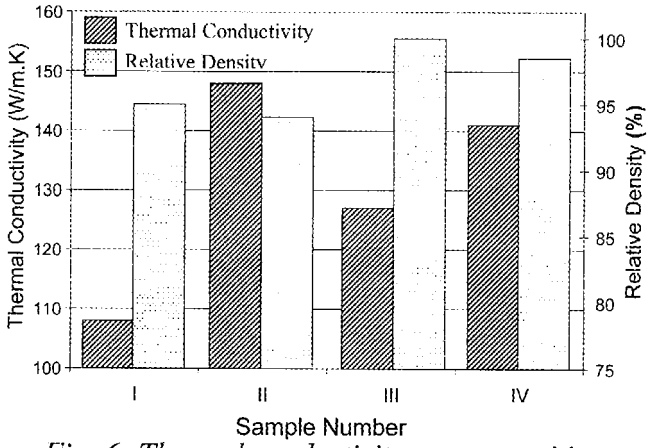

Fig. 6: Thermal conductivity vs. composition.

Furthermore, it was shown by the experimental work of Medraj *et al.* [10] that YAP wets the surface of AlN more than YAG or YAM if all the experimental conditions are considered. Hence the presence of YAP phase will prevent AlN-AlN surface contact. For this reason the thermal conductivity of compositions II, III and IV varies according to the amount of YAP phase. As discussed above, compositions II, III and IV have 1.39, 2.95 and 1.84 wt% YAP, respectively, and the corresponding values of thermal conductivity are 148, 127 and 141 W/m.K, respectively. Hence higher YAP content is associated with lower thermal conductivity.

Conclusions

- An optimized self-consistent thermodynamic database has been developed for AlN- Al_2O_3-Y_2O_3 with the computer software F*A*C*T. This database can now be used to predict the phase relations and various thermodynamic properties in this three-component system, which represents the sintering of AlN.
- High temperature neutron diffractometry has permitted real time reaction studies in the AlN-Al_2O_3-Y_2O_3 system, especially to determine the temperature range of each reaction, which would have been impossible by any other means.
- Thermodynamic modeling of the AlN-Al_2O_3-Y_2O_3 system provides an important basis for understanding the sintering behaviour of aluminum nitride, and explains the experimental results:
  - Samples with higher density have lower liquid formation temperature.
  - Thermal conductivity is related to the chemistry of the secondary phases.
  - Samples with residual Al_2O_3 and/or γ-spinel have lower thermal conductivity.
  - Thermal conductivity decreases with the increasing amount of the YAP phase, because YAP wets the AlN surface and prevents AlN-AlN grain boundary formation.
- AlN can be sintered to full density both with and without additive using compositional control. However, the Y_2O_3 additive reduces the sintering temperature and plays an important role in the microstructural development.

Acknowledgments

This study was carried out with the support of an NSERC Strategic Project grant. The authors are indebted to the opportunity provided by NPMR-NRC in Chalk River to conduct the high temperature *in situ* neutron diffraction experiments and Y. Baik for providing some of the sintering data.

References

[1] N. H. Kim, K. Komeya and T. Meguro: Effect of Al_2O_3 Addition on Phase Reaction of AlN-Y_2O_3 System. *J. Mater. Sci*, 31[6], 1996, 1603-1608.

[2] M. Hotch: Calculation of Ternary, Quaternary, and Higher-Order Phase

Diagrams from Binary Diagrams and Binary Thermodynamic Data. *J. Phase Equilibria*, 14[6], 1993, 710-717.

[3] C. W. Bale, A. D. Pelton and W. T. Thompson: Facility for the Analysis of Chemical Thermodynamics. McGill University/Ecole Polytechnique, 1996.

[4] M. Medraj, R. Hammond, W.T. Thompson and R.A.L. Drew: Thermodynamic Modeling of the AlN-Al_2O_3-Y_2O_3 System. *Can. Metall. Q.*, 42[4], 2003, 495-506.

[5] M. Medraj, R. Hammond, W.T. Thompson and R.A.L. Drew: High Temperature Neutron Diffraction of AlN-Al_2O_3-Y_2O_3 System. *J. Am. Ceram. Soc.*, 86[4], 2003, 717-726.

[6] J. Cheng, D. Agrawal and R. Roy: Microwave Synthesis of Aluminum Oxynitride (ALON). *J. Mater. Sci. Lett.*, [18], 1999, 1989-1990.

[7] L. Yawei, L. Nan and Y. Runzhang: The Formation and Stability of γ-Aluminum Oxynitride Spinel in the Carbothermal Reduction and Reaction Sintering Processes. *J. Mat. Sci.*, [32], 1997, 979-982.

[8] R. A. L. Drew, Y. Baik and M. Entezarian: Effect of Y_2O_3 Content on Sintering of Aluminum Nitride, *Mater. Sci. Forum.*, [325-326], 2000, 249-254.

[9] T. B. Jackson, A. V. Virkar, K. L. More, R. B. Dinwidie and R. A. Cutler: High-Thermal Conductivity Aluminum Nitride Ceramics: The Effect of Thermodynamic, Kinetic, And Microstructure Factors. *J. Am. Ceram. Soc.*, 80[6], 1997, 1421-1435.

[10] M. Medraj, M. Entezarian and R. A. L. Drew: Wettability of Al_2O_3-Y_2O_3 compounds on Aluminum Nitride and Their Role in Sintering. *Sintering 99 Conference Proceedings*, 2000, 307-312.